Recovery of iron by jarosite crystallization and separation of vanadium by solvent extraction with extractant 7101 from titanium white waste liquid (TWWL)

Wang Li, Zepeng Niu and Xiaobo Zhu

ABSTRACT

The jarosite crystallization and new extractant system for extractant 7101 was used to separate iron and extract vanadium from titanium white waste liquid (TWWL). The influence factors and mechanisms of crystallization and solvent extraction were investigated and analyzed using SEM-EDS, XRD, FT-IR, solution thermodynamic theory and extraction isothermal curve. More than 97% of iron was precipitated with the following conditions: potassium chlorate 15 g/L, pH value of 1.6, temperature of 95 °C and time of 90 min, in which the crystallization product was jarosite with a purity of 99.5%; the pH value of the solution decreased after precipitation. The extraction efficiency of vanadium reached 88.6% with 10% Fe, 5% Al(III) but less for Mg(II), K(I) and Na(I) under the conditions X_{7101} of 0.5, pH value of 2.0, time of 4 min and stirring speed of 40 r/min. The extraction of metal ions occurred in the order V(V) > Fe(III) > Al(III) > Mg(II) > K(I). Vanadium minimally existed as $H_2V_{10}O_{28}^{4-}$ at pH 2.0, and the functional groups NH and C–N contributed to vanadium extraction using the extractant 7101. Four stages extraction and three stages of re-extraction were predicated by McCable–Thiele plots.

Key words | crystallization, extractant 7101, iron, jarosite, solvent extraction, vanadium

Wang Li
Zepeng Niu
Xiaobo Zhu (corresponding author)
College of Chemistry and Chemical Engineering,
Henan Polytechnic University,
Jiaozuo Henan 454000,
China
E-mail: *zhuxiaobo0119@163.com*

Xiaobo Zhu
Collaborative Innovation Center of Coal Mine Safety of Henan Province,
Henan Polytechnic University,
Jiaozuo Henan 454000,
China
and
State Environmental Protection Key Laboratory of Mineral Metallurgical Resources Utilization and Pollution Control,
Wuhan University of Science and Technology,
Wuhan Hubei 430081,
China

HIGHLIGHTS

- Crystallization and solvent extraction were studied for separation of Fe and V.
- Separation mechanism of Fe and V from TWWL was detected by thermodynamic analysis.
- Removal and recovery process of Fe and V was analyzed by XRD, SEM-EDS and FT-IR.

INTRODUCTION

The titanium white waste liquid (TWWL) is a waste acid from the industrial production of titanium white from vanadium titano-magnetite by physical separation, sulfuric acid leaching and hydrolysis precipitation (Wei *et al.* 2007; Cui & Ren 2013; Li & Dai 2014; Song & Wang 2019). It is estimated that 8 tons of 20% TWWL are produced for every ton of titanium dioxide. TWWL can cause environmental pollution due to its high acidity and high content of metal ions such as iron and vanadium (Liu *et al.* 2016; Yu 2017; Yuan 2017; Hu *et al.* 2020).

At present, treatment of TWWL mainly includes three methods: the neutralization method, the re-use of the residual acid, and the comprehensive recovery of the valuable metals (Zhao *et al.* 2005; Xie *et al.* 2016; Li *et al.* 2018a, 2018b; Zhou *et al.* 2020). In the neutralization method, the treated wastewater is discharged with a pH value of 6–8 by the addition of lime, limestone, soda, caustic soda, and other alkaline substances. Although the pH value of the wastewater conforms to regulations, the wastewater produces a large amount of industrial waste residue. The residue is more difficult to deal with and the valuable metals are not recovered (Zhang *et al.* 2014). In the recovery and re-use of the residual acid, the process of purification, diffusion, and vacuum concentration is carried out, which increases the acid

doi: 10.2166/wst.2021.114

concentration by 65% (Yang *et al.* 2015; Liu *et al.* 2017; Feng *et al.* 2018). Furthermore, acid leaching for recovery of valuable metals from solid mineral resources such as red mud, vanadium-bearing steel slag and LD converter slag was investigated by directly using TWWL (Tang *et al.* 2010; Zhang *et al.* 2015, 2021), but iron also dissolved into the leaching solution, resulting in a difficult separation and purification of vanadium from the acid solution.

Therefore, separation and purification were necessary for removal of iron and recovery of vanadium from TWWL. Common methods including ion exchange, solvent extraction and activated carbon adsorption have been applied for separation of iron and vanadium (Xing *et al.* 2021). Solvent extraction has been widely applied for the high concentration sulfuric acid system (Li *et al.* 2012; Peng *et al.* 2019). Many researchers have promoted solvent extraction for separation of vanadium using cyanex301, DEHPA, cyanex272, amyl acetate, P204, TBP, P507, N1923 and Cyphos IL 101 from acid solution. However, iron ions were especially detrimental to the subsequent separation and purification of vanadium by solvent extraction (Jiang *et al.* 2015; Shi *et al.* 2017; Zhu *et al.* 2019). Although sodium sulfite was used to reduce Fe^{3+} to Fe^{2+} to avoid co-extraction of Fe^{3+}, some Fe^{2+} ions were still extracted due to the high concentration of iron ions (Li *et al.* 2011). Therefore, it is important to remove iron ion before the solvent extraction of vanadium from TWWL using the precipitation method (Hu *et al.* 2017; Wang *et al.*, 2020a, 2020b).

Precipitation using jarosite was tried to due to many sulfate and iron ions in the TWWL. The jarosite process is an important method to separate iron from other metals in acid solutions with high iron concentrations and has been widely applied in the Cu, Mn and Sn industries (Liu *et al.* 2019; Lu *et al.* 2020; Rabbani & Ahmadi 2020). For the solution of precipitated iron, the new solvent extraction agents including 7101 and sec-octyl alcohol were used to separate vanadium. The influence of potassium chlorate dosage, pH value, reaction temperature, and reaction time on the efficient comprehensive recovery of iron and separation of vanadium was determined. The extracting selectivity of the extractants was also studied under the different conditions of X_{7101}, pH value, time and stirring speed in this work. The separation mechanism for iron and vanadium was analyzed using XRD, SEM-EDS, FT-IR, solution thermodynamics and extraction isothermal curve. Therefore, the research was investigated to effectively recover iron and separate vanadium from TWWL, which may provide a new approach and method for comprehensive use of TWWL.

EXPERIMENTAL

Materials

The chemical composition of TWWL is shown in Table 1.

Potassium chlorate, potassium hydroxide, Sulfuric acid, extractant 7101, P204, N235, Cyanex272, sec-octyl alcohol, kerosene and ammonium carbonate and other agents with analysis pure were purchased from Kechuang Reagent Co. Ltd. The sulfonated process was carried out before the use of kerosene. The kerosene and concentrated sulfuric acid were mixed and stirred twice, in which the volume ratio of kerosene and sulfuric acid was 5:1. The olefins and alkaline compounds containing nitrogen were removed by stirring for 10 minutes. Kerosene was washed with 5% sodium carbonate solution with the O/A volume ratio of 5:1 to remove excess sulfuric acid and acidic compounds in the kerosene. Finally, the kerosene was washed with distilled water and the transparent sulfonated kerosene was obtained.

Methods

TWWL (100 mL) was mixed with potassium chlorate and stirred for 30 min using a magnetic stirrer. Then, the solution was adjusted to a suitable pH with KOH. Next, potassium hydroxide was dissolved into the solution, which was stirred under different temperature and time regimes. The jarosite precipitate appeared and was filtered from the solution.

The organic phase containing extractants and sulfonated kerosene was mixed and obtained according to ratio requirements. Firstly, the 50 mL solution of precipitated iron was adjusted to appropriate pH value and put into a 250 mL conical flask. Then, the organic phase was also put into the conical flask and the conical flask was put on an oscillator. Several experiments were carried out under different conditions of different pH value, $X_{extractant}$, extraction time and stirring speed. The mixture in the conical flask was put into a separating funnel and left to stand for 5 min. The raffinate was discharged from the separating funnel by opening the valve. The loaded organic phase was still used to extract vanadium from the new solution until the organic phase was saturated.

Table 1 | Chemical composition of leaching solution

Element	Al	Fe^{2+}	Fe^{3+}	V	Mg
Concentration (g/L)	1.71	17.42	3.24	0.54	2.18

Analysis process

Element content in the TWWL, solution of precipitated iron and raffinate was detected using an Inductively Coupled Plasma Optical Emission Spectrometer (ICP-OES, iCAP 7000 Plus, China). Solution thermodynamics of vanadium and iron was analyzed using HCS software. Analysis of the extractant and loaded extractant was carried out using the Fourier transform infrared spectroscopy (FT-IR, NIR256, The Netherlands). The crystallization efficiency of iron and other metals was calculated using Equation (1):

$$\eta = (b - a)/b \times 100\% \quad (1)$$

where η is the crystallization efficiency of the metals (%), a is the content of metals in the solution of precipitated iron (g), and b is the content of metals in the leaching solution (g).

The extraction efficiency of metal, distribution coefficient and separation factor were calculated using Equations (2)–(4), respectively:

$$\gamma = \frac{(CV - C_0V_0)}{CV} \quad (2)$$

$$D = C_1/C_0 \quad (3)$$

$$\beta = D_{(V)}/D_{(metal)} \quad (4)$$

where γ is the extraction efficiency of metal (%), V_0 is volume of raffinate (L), C_0 is the metal concentration of raffinate (g/L), V is volume of solution of precipitated iron (L), C is the metal concentration of solution of precipitated iron (g/L), C_1 is the metal concentration of organic phase (g/L), D is the distribution coefficient of metal (%), and β is separation factor of vanadium and other metal.

RESULTS AND DISCUSSION

Recovery of iron from TWWL

Effect of potassium chlorate concentration and pH value

The effect of the potassium chlorate concentration on the crystallization efficiency of iron and other metals was investigated with different pH values at 95 °C for 90 min. The result is shown in Figure 1.

Figure 1 shows that the potassium chlorate dosage and the pH value significantly affected the crystallization efficiency of iron and the pH value of the processed solution. The precipitation efficiency of iron increased with the increase in the potassium chlorate concentration at a pH value of 1.0, but the precipitation efficiency of other metals was negligible and the pH value of the precipitated liquid decreased. The precipitation efficiency of iron was 25% when using 5 g/L potassium chlorate and increased to 61% when increasing the potassium chlorate dosage to 20 g/L without any precipitation of other metals. At the same time, the higher iron precipitation efficiency caused a lower pH value of the solution after precipitation. The pH value of the processed solution decreased from 1.0 to 0.7. The precipitation efficiency of iron also increased with the potassium chlorate concentration at a pH value of 1.3. The precipitation efficiency of iron increased from 31% to 79% with an increase in potassium chlorate from 5 to 20 g/L, in which the precipitation efficiency of other metals was also negligible. However, the precipitation efficiency of iron was 59% with 5 g/L potassium chlorate. The precipitation efficiency of iron reached 97% by increasing the potassium chlorate dosage to 15 g/L at a pH of 1.6, in which the precipitation efficiency of Al was about 3%. The precipitation efficiency of iron increased relatively slowly with the potassium chlorate concentration at a pH value of 1.9 The precipitation efficiency of iron was 82% with 5 g/L potassium chlorate. The precipitation efficiency of iron reached 99% by increasing the potassium chlorate dosage to 20 g/L. The formation of jarosite required Fe^{3+}, K^+ and SO_4^{2-} ions under suitable concentration ratio of ions and pH value (Calla-Choque & Lapidus 2021). Iron mainly existed as Fe^{2+} in the TWWL and must be oxidized to Fe^{3+}. Potassium chlorate was chosen as the oxidant considering that a certain amount of potassium ion was needed in the jarosite formation process. Considering the requirements of reagent consumption and precipitation efficiency of iron, the suitable pH value of 1.6 and the potassium chlorate dosage of 15 g/L were selected.

Effect of reaction temperature and time

The effect of the reaction temperature and the reaction time on the crystallization efficiency of iron was investigated with 15 g/L potassium chlorate at a pH of 1.6. The result is shown in Figure 2.

Figure 2 indicates that the reaction temperature significantly affected the crystallization efficiency of iron. The crystallization efficiency of iron increased with an increase in reaction temperature. Efficiency increased from 1% to 42% when the reaction temperature was increased from

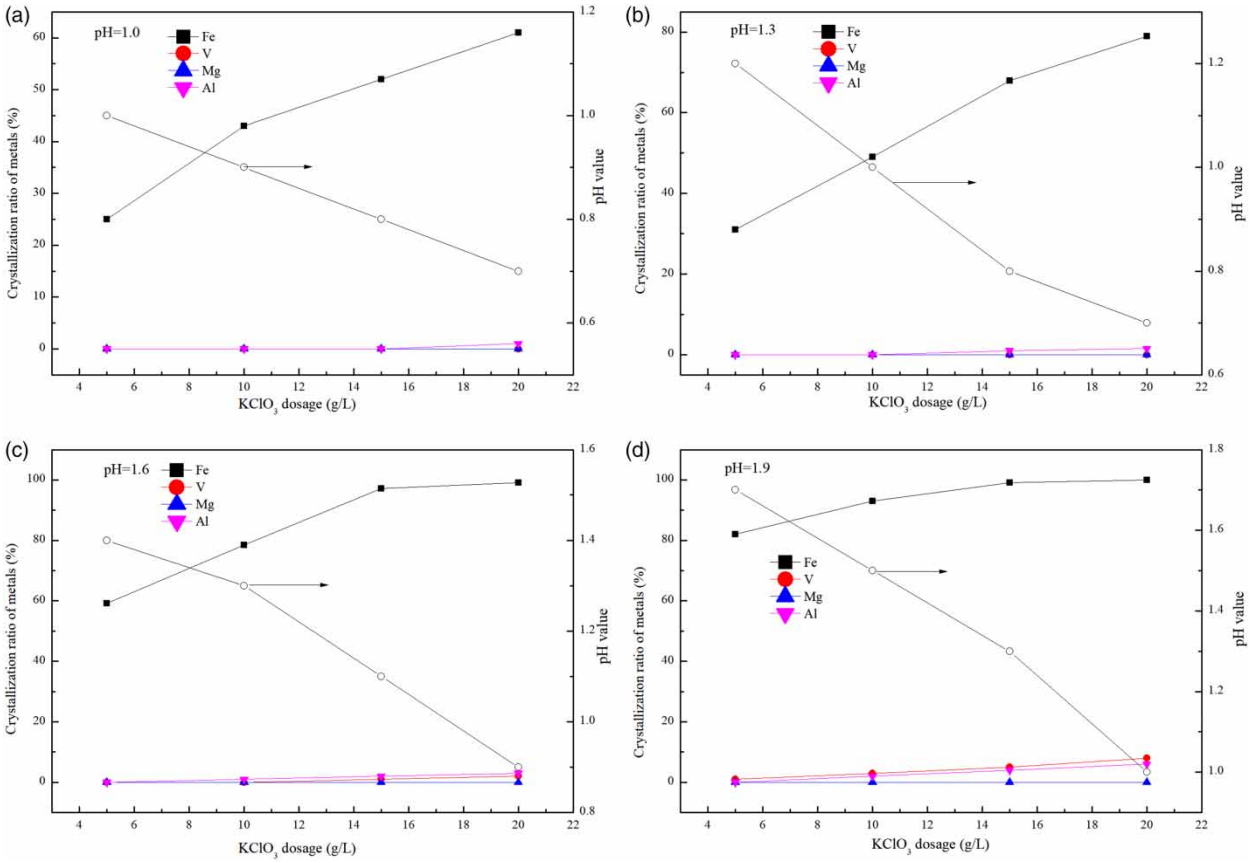

Figure 1 | Effect of $KClO_3$ dosage on crystallization of metals at different pH values.

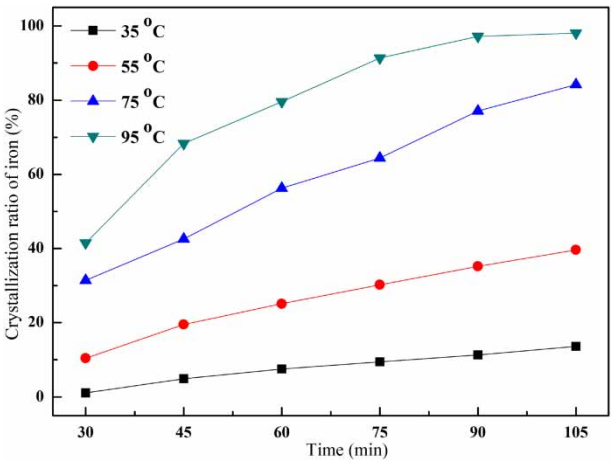

Figure 2 | Effect of temperature and time on crystallization of iron.

35 °C to 95 °C for a duration of 30 min. The crystallization efficiency of iron increased from 8% to 80% by increasing the reaction temperature from 35 °C to 95 °C for 60 min. The crystallization efficiency of iron increased from 11% to 97% when the reaction temperature was increased from 30 °C to 90 °C for 90 min. Reaction time also significantly affected the crystallization efficiency of iron at high reaction temperatures, whereas it only slightly increased with the reaction time at low temperatures. Crystallization efficiency of iron increased from 1% to 11% when the reaction time was increased from 30 to 90 min at 35 °C. Crystallization efficiency of iron increased from 42% to 97% when the reaction time was increased from 30 to 90 min at 95 °C. A higher precipitation efficiency was achieved by increasing the reaction time at high temperatures. Typically, the crystallization efficiency of iron reached 97% for potassium chlorate concentration of 15 g/L, pH value of 1.6, reaction temperature of 95 °C, and reaction time of 90 min. Temperature is a key factor for the precipitation efficiency of iron. The precipitation efficiency of iron was generally high with an increase of temperature, which was determined by the thermodynamic characteristics of jarosite precipitation (Li *et al.* 2018a, 2018b). The precipitation process was a process of nucleation formation and growth, which needed a certain time to fully complete the reaction. the precipitation rate of

iron was higher with longer time according to kinetic characteristics (Baccolo *et al.* 2021).

Crystallization performance and analysis of the product

A crystallization product was obtained with 15 g/L potassium chlorate at a pH of 1.6 at 95 °C for 90 min. Granules were small and scattered. The SEM-EDS and XRD results for the product are shown Figure 3.

Figure 3 shows that the crystallization product was jarosite, in which the main elements in the crystallization product were oxygen, sulfur, potassium, and iron with small amounts of carbon, titanium, aluminum, and calcium. Accordingly, the product was identified as jarosite with a purity of 99.5% by the analysis results from ICP-AES.

Separation mechanism of iron

The thermodynamics diagram for the iron solution is shown in Figure 4.

Iron mainly exists as an elementary substance low potential conditions. The elementary substance was gradually oxidized as the ions of Fe(II) ions with increase in potential at pH 0 to 6. Precipitation of ferrous iron takes place in alkaline conditions. Fe(II) ion was gradually oxidized to Fe(III) with continuing improvement in potential value of the solution. Fe(III) was stable under conditions of strong acid with pH values 0 to 1.9. Usually, a precipitate with Fe(III) was formed at pH values >1.9 according to the thermodynamics analysis. The precipitation of ferric iron hydroxide took place with increase the solution pH value.

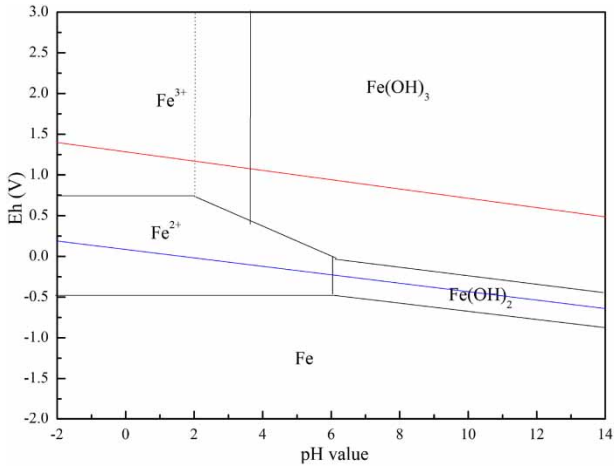

Figure 4 | Thermodynamics diagram for the iron solution.

The precipitation products of iron hydroxide were almost fully processed at a pH value of 3.5. The mixed ions of Fe(II) and Fe(III) are stable between the forms O_2/H_2O and H_2O/H_2 under normal condtions, which was consistent with the results of iron ion morphology in the TWWL.

However, jarosite is a compound salt according to our study (Li *et al.* 2018a, 2018b). Jarosite started to precipitate at pH 1.0 and complete precipitation occurred at pH 1.9, in which the oxidation reaction of Fe^{2+} could be carried out using $KClO_3$ into the leaching solution (Equation (5)):

$$6H^+ + 6Fe^{2+} + ClO_3^- = 6Fe^{3+} + Cl^- + 3H_2O \quad (5)$$

Temperature was the key factor for the precipitation efficiency of jarosite, in which a temperature of 95 °C was

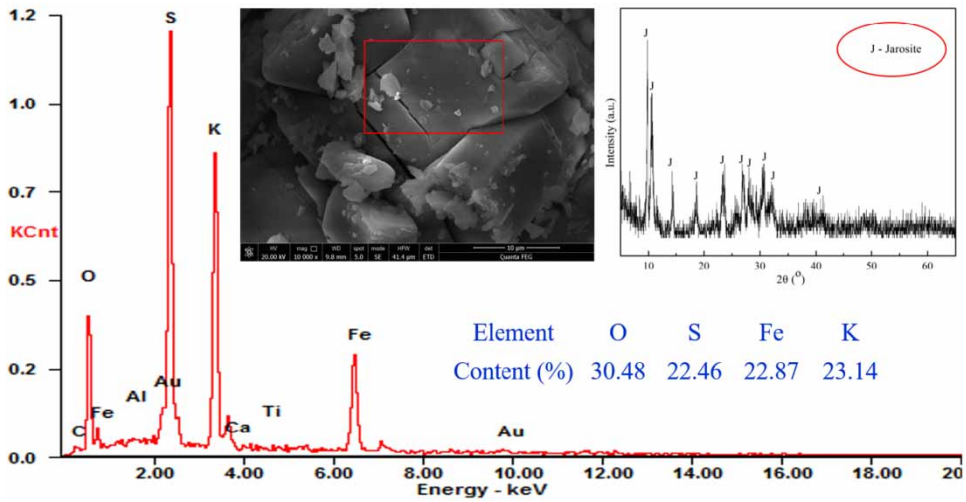

Figure 3 | SEM-EDS and XRD pattern of the product.

necessary for a full reaction. Gibbs free energy of potassium, iron, and sulfuric acid in the solution was obtained from the following equations:

$$2K^+(aq) + SO_4^{2-}(aq) = K_2SO_4(s) \quad (6)$$

$$2Fe^{3+}(aq) + 3SO_4^{2-}(aq) = Fe_2(SO_4)_3(s) \quad (7)$$

$$K^+(aq) + 3Fe3^+(aq) + 2SO_4^{2-}(aq) + 6H_2O(aq) = KFe_3(SO_4)_2(OH)_6(s) + 6H^+(aq) \quad (8)$$

Figure 5 shows the Gibbs free energy change at different temperatures by calculation. Gibbs free energy of potassium sulfate increased with an increase in temperature. When the temperature was higher, the solid was more difficult to obtain in the solution as the solubility of potassium sulfate increased with the reaction temperatures. Gibbs free energy of jarosite began less than 0 at 355 K, which indicates that the reaction could spontaneously occur at this temperature. The Gibbs free energy of reaction was lower at higher temperature. Furthermore, generation of jarosite provided some hydrogen ions according to Equation (5), which was consistent with the experimental results.

Solvent extraction of vanadium

Effect of extractants on separation of vanadium and iron

The chemical composition of precipitated solution is shown in Table 2.

Table 2 | Chemical composition of precipitated solution

Element	V	Al	K	Fe^{3+}	Mg
Concentration (g/L)	0.52	1.69	2.64	0.62	2.17

The effect of typical extractants P204, 7101, N235 and Cyanex272 on extraction efficiency of vanadium and iron was investigated, and the result is shown in Figure 6.

The extraction efficiency of vanadium was more than 80% using P204 or 7101, respectively at pH 2.0, whereas the extraction efficiency of vanadium was 60%–70% when using extractant N235 or Cyanex272. It should be noted that P204 has an obvious synergistic effect with iron, and the extraction efficiency of iron was close to 40%. The synergistic extraction efficiency of iron with N235 or Cyanex272 was 15%–20%. The extraction efficiency of iron was 10% when using extractant 7101, which was a suitable extractant for extraction of vanadium and separation of iron. RNH_2 from the extractant 7101 may change to $RNH_3(HSO_4)$ in sulfuric acid, and could extract the anions from the acid solution. The extractants were important factors affecting the recovery of vanadium. The extraction effect of vanadium was different due to various exchange functional groups of extractants (Liu *et al.* 2020a, 2020b). The V(V) form exists in the TWWL and existed in the anion form according to the following solution thermodynamics research on vanadium. Therefore, extractant 7101 was effective for extracting vanadium due to its anion exchange functional group.

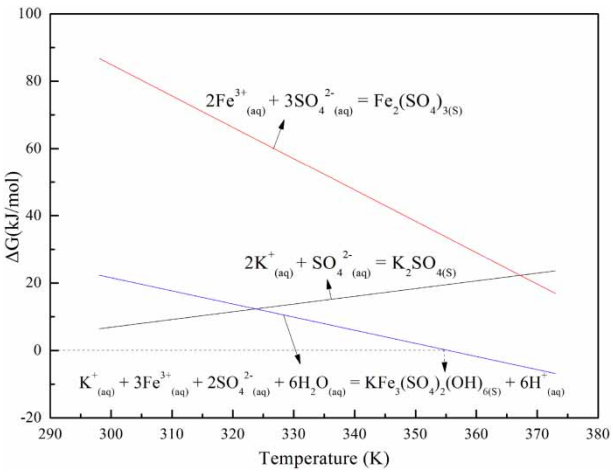

Figure 5 | Gibbs free energy diagram of the formation reaction.

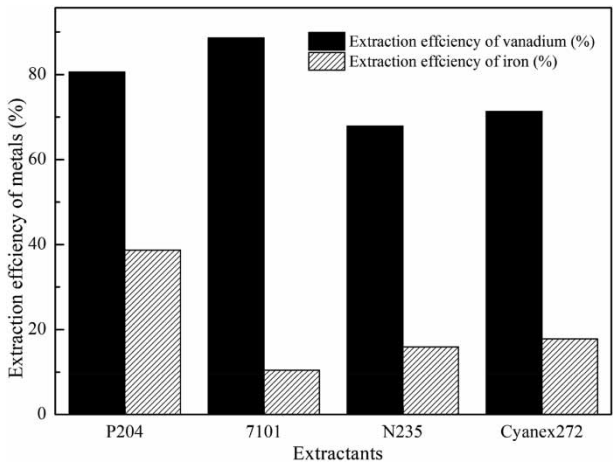

Figure 6 | Effect of extractant 7101 on extraction efficiency of vanadium and iron. Experimental conditions: pH = 2.0 ± 0.05, O/A = 1:1, [extractants]/[Sulphonated kerosene] = 20:80 (v/v), time = 4 min, stirring speed = 40 r/min.

Extraction of V(V) with a mixture of extractant 7101 and sec-octyl alcohols

Solvent extraction of V(V) from the precipitated solution was carried out with extractant 7101 and sec-octyl alcohols at pH 2.0 ± 0.05.

Figure 7 shows that the effect of extractant 7101 volume fraction in extractant (X_{7101}) on the extraction efficiency of vanadium and distribution coefficient $D_{(V)}$. It is suggested that 7101 mixed with sec-octyl alcohol was beneficial for extracting vanadium from the solution. The maximum distribution coefficient (Dv = 7.77) was obtained at $X_{7101} = 0.5$, which means that 10% 7101 and 10% sec-octyl alcohol was mixed with 80% sulfonated kerosene. The extraction efficiency of vanadium reached 88.6% at $X_{7101} = 0.5$. Compared with extraction using pure 7101 ($X_{7101} = 1.0$) and sec-octyl alcohol ($X_{7101} = 0$) alone, 78.6% and 2.4% of vanadium was obtained, respectively. The main component of vanadium extraction was extractant 7101 and sec-octyl alcohol had a lesser extraction effect on vanadium. Co-extractants were widely used in the solvent extraction process, which could improve the solubility of main extractant in organic phase and assist the separation of two phases (Guo *et al.* 2020). The sec-octyl alcohol can effectively improve the extraction performance of 7101 and increase the solubility of the extraction compound in the kerosene. The organic phase was viscous and the interface between the two phases was unclear without the addition of sec-octanol.

The effect of various concentrations of organic phase (7101 + sec-octyl alcohol) is shown in Figure 8.

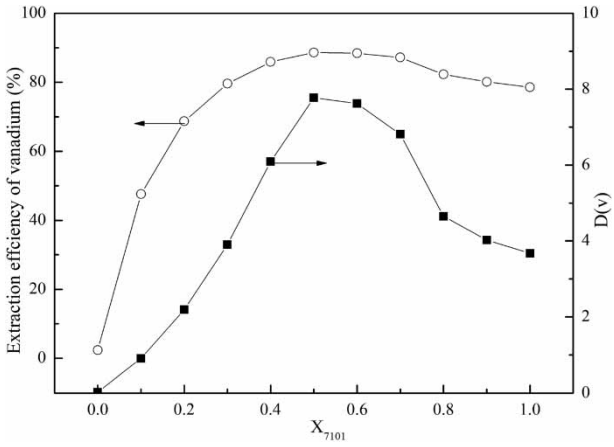

Figure 7 | Extraction of vanadium with a mixture of extractant 7101 and sec-octyl alcohols. Experimental conditions: pH = 2.0 ± 0.05, O/A = 1:1, [extractant 7101+ sec-octyl alcohols]/[Sulphonated kerosene] = 20:80 (v/v), time = 4 min, stirring speed = 40 r/min.

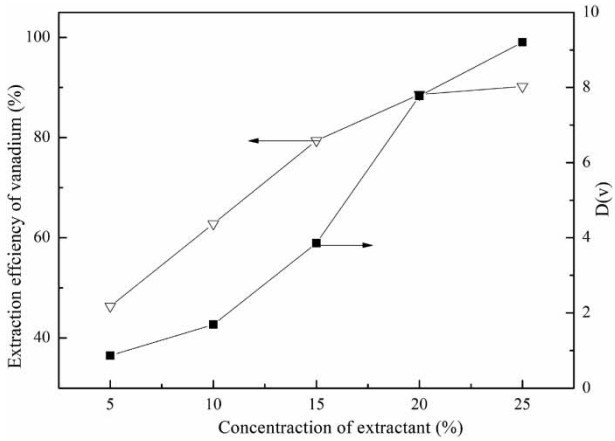

Figure 8 | Effect of extractant concentration on recovery of vanadium with extractant 7101 and sec-octyl alcohols. Experimental conditions: pH = 2.0 ± 0.05, [extractant 7101]:[sec-octyl alcohols] = 10:10 (v/v), O/A = 1:1, time = 4 min, stirring speed = 40 r/min.

The extraction efficiency of vanadium increased with an increase in the organic phase concentration. The extraction efficiency of vanadium increased significantly from 46.4% to 88.6%. with an increase in the organic phase concentration from 5% to 20%. The extraction efficiency of vanadium only increased to 90.2% with the organic phase concentration of 25%. The useful functional groups of the extractant were generally easily bound to vanadium with a leaching solution with a higher concentration of extractant, so the extraction efficiency of vanadium increased with increase in extractant concentration (Feng *et al.* 2021). Therefore, 10:10 (7101:sec-octyl alcohol and 20% organic phase were selected to extract and separate vanadium from the solution of precipitated iron.

Selective extraction of vanadium from foreign ions with extractant 7101 and sec-octyl alcohol

To verify the selectivity of extractant 7101, vanadium and other metals ions were extracted at different pH values from the leached liquid. The extraction efficiency of metals and the separation factor (β) are shown in Figure 9.

The results indicated that the extraction of metal ions occurred in the order V(V) > Fe(III) > Al(III) > Mg(II) > K(I). The extraction efficiency of vanadium increased as the solution pH was increased from 1.6 to 2.2. However, the extraction efficiency of vanadium slightly decreased at pH was 2.4. The extraction efficiency of Fe(III) increased as the solution pH was increased from 1.6 to 2.4. Extraction efficiency of Al(III) was about 5%, whereas the extraction efficiencies of Mg(II) and K(I) were negligible (0–3%) with

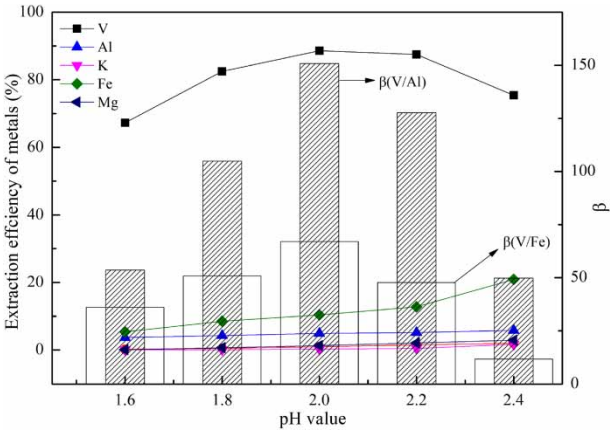

Figure 9 | Effect of pH value on extraction and separation of vanadium and foreign ions. Experimental conditions: [extractant 7101]:[sec-octyl alcohols] = 10:10 (v/v), [extractant 7101+ sec-octyl alcohols]/[Sulphonated kerosene] = 20:80 (v/v), O/A = 1:1, time = 4 min, stirring speed = 40 r/min.

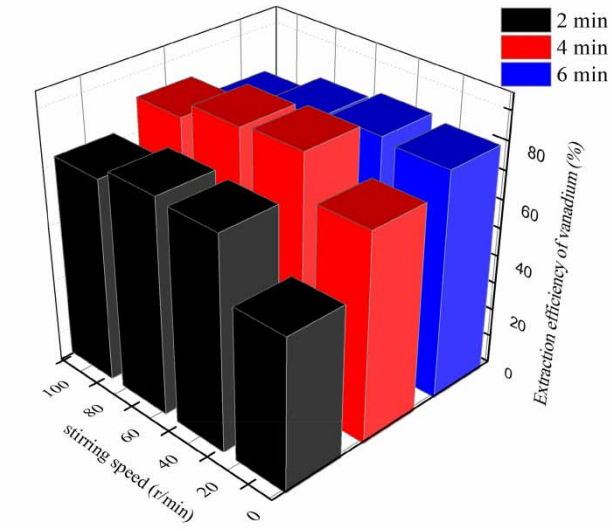

Figure 10 | Effect of stirring speed and time on extraction of vanadium. Experimental conditions: [extractant 7101]:[sec-octyl alcohols] = 10:10 (v/v), [extractant 7101+ sec-octyl alcohols]/[Sulphonated kerosene] = 20:80 (v/v), O/A = 1:1, pH = 2.0 ± 0.05.

the organic phase of extractant 7101 and sec-octyl alcohol. It is worth noting that the emulsification occurred in the extraction process and many three-phase substances were formed at the phase interface at pH value more than 2.2. The emulsification may be caused by the precipitation with the hydrolysis of iron ions and mixing the organic phase, which resulted in a decrease in vanadium extraction efficiency (Liu *et al.* 2020a, 2020b). The separation factor (β) is an important parameter for estimating the selectivity of extractant. Based on the extraction efficiency of metal ions, the β value of V with Al and Fe was 150 and 67, respectively, with the organic phase of extractant 7101 and sec-octyl alcohol at pH = 2.0, which indicates that the extraction of vanadium was easier than Al and Fe. In conclusion, the selective extraction of vanadium from Al and Fe was obtained by solvent extraction with extractant 7101 and sec-octyl alcohol.

Effect of stirring speed and time on extraction of vanadium

Experiments were carried out to discuss the effect of stirring speed and time on the extraction of vanadium with extractant 7101 and sec-octyl alcohols.

The results from Figure 10 show that vanadium extraction can reach an equilibrium at 4 min with stirring speed of 40 r/min. However, the extraction efficiency of vanadium had a tendency to decrease over 6 min at the same oscillation rate, in which the emulsification of organic phase occurred leading to the partial failure of the organic phase. Furthermore, the stirring speed should not be excessively fast, which could also lead to emulsification (Wang *et al.*, 2020a, 2020b). Extraction efficiency of vanadium decreased due to the third phase in the extraction process with a stirring speed of 70 r/min. Therefore, 4 min and 40 r/min were the optimal time and stirring speed for extraction of vanadium.

FT-IR analysis of organic phases

The FT-IR spectra of the organic phase and loaded organic phase were detected and compared to determine the extraction mechanism. The result is shown in Figure 11.

Sulfonated kerosene is a mixture of alkanes, in which the stretching vibration absorption of C–H existed at 2,954, 2,921 and 2,853 cm^{-1}. The stretching vibration peak of C ≡ C was present at 2,131 cm^{-1}, which was the characteristic peak of kerosene following an inadequate sulfonation process. The bending vibration peak of CH was present at 1,485 and 1,377 cm^{-1} in the sulfonated kerosene. The bending vibration peak of NH was present at 796 and 722 cm^{-1} in the primary amine 7101. New vibration peaks were present in the organic phase after extraction of vanadium, in which the skeleton of primary amine 7101 and sulfonated kerosene was changed. The bending vibration peak for NH was present at 1,622 cm^{-1}. The bending vibration peak of NH and stretching vibration absorption of –C–N were present at 1,537 cm^{-1}. Furthermore, the stretching vibration absorptions of C–O and C–N were present at 1,189 and

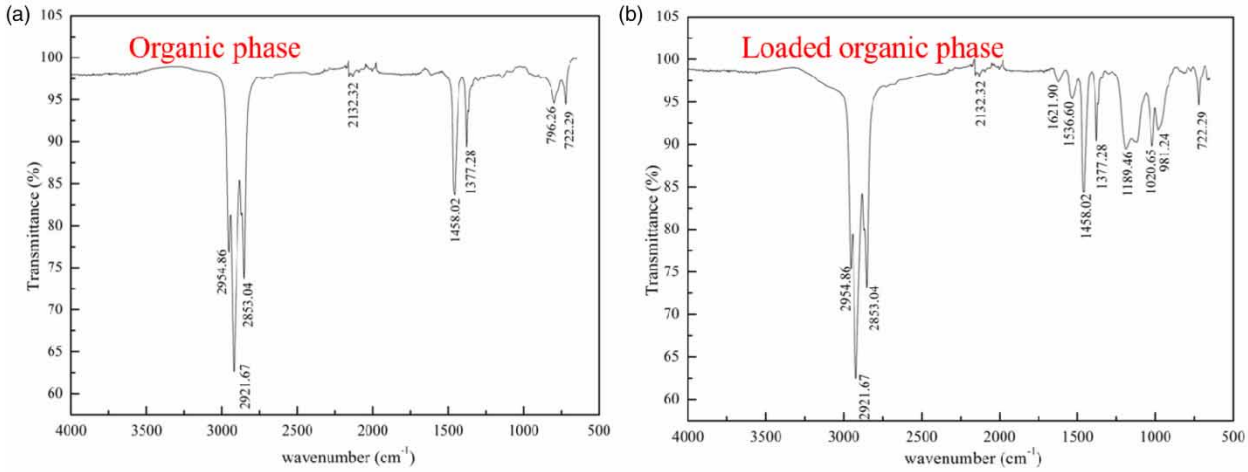

Figure 11 | FT-IR spectra of extractant 7101 and loaded organic phase.

1,021 cm^{-1} due to the extraction of vanadium into the primary amine 7,107.

Thermodynamic analysis of vanadium

The Eh-pH graph for vanadium under standard conditions was analyzed and shown in Figure 12 according to the thermodynamic data of Gibbs free energy of vanadium in solution.

Vanadium can dissolve into the solution and is present as a cation only under acidic conditions of V(II) and V(III). The oxide of V(IV) belongs to an amphoteric oxide, which could dissolve into acid solution and alkaline solution. VO^{2+} can exist in acid solution following dissolution of VO_2. It can also exist in the form $HV_2O_5^-$ under alkaline conditions. The oxide of V(V) was relatively complex, in which VO_2^+ was stable under strongly acidic conditions of pH <1.0. Various forms of anion are present with the dissolution of V_2O_5 at pH value >1.0, in which the forms $H_2V_{10}O_{28}^{4-}$, $HV_{10}O_{28}^{5-}$, $HV_6O_{17}^{3-}$, $H_3V_2O_7^-$, HVO_4^{2-} and VO_4^{3-} exist. The pH value of the precipitated solution was adjusted to 2.0 before the extraction process, so vanadium was almost present as $H_2V_{10}O_{28}^{4-}$ at pH values from 1.0 to 2.0, and was beneficial to improve the extraction efficiency of vanadium using extractant 7101. However, iron was mostly present in the form of cations under these conditions. Therefore, the selective extraction of vanadium and separation of impurity cations were achieved by using extractant 7101, which can be represented by Equation (9):

$$(RNH_3)HSO_4 + H_2V_{10}O_{28}^{4-} \rightarrow (RNH_3)_4H_2V_{10}O_{28} + 4HSO_4^- \quad (9)$$

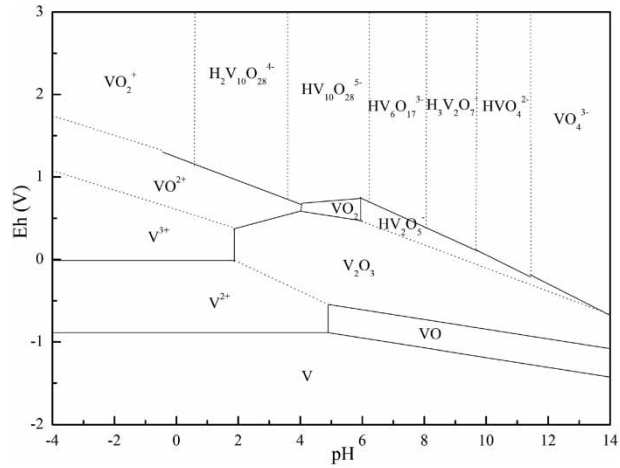

Figure 12 | Eh-pH diagram of vanadium in the solution.

The counter-current simulation experiments

The vanadium extraction isotherm was carried out to determine the number of stages using 10% 7101 (v/v), 10% sec-octyl alcohol and 80% sulfonated kerosene with different O/A from 1:0.5 to 1:20 at pH value of 2.0 for 4 min. The McCabe-Thiele diagram for extraction of vanadium is indicated in Figure 13.

Four theoretical extraction stages should be needed at O/A ratio of 1:5. Therefore, the four stages in the counter-current simulation experiments were carried out, and the chemical composition of the raffinate is shown in Table 3.

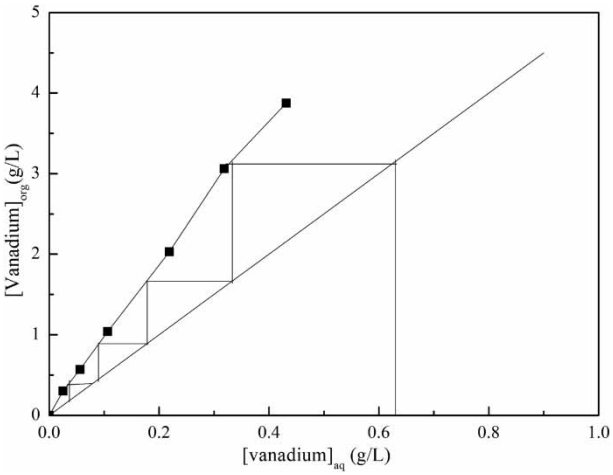

Figure 13 | McCable–Thiele plot for extraction of vanadium with extractant 7101 and sec-octyl alcohols.

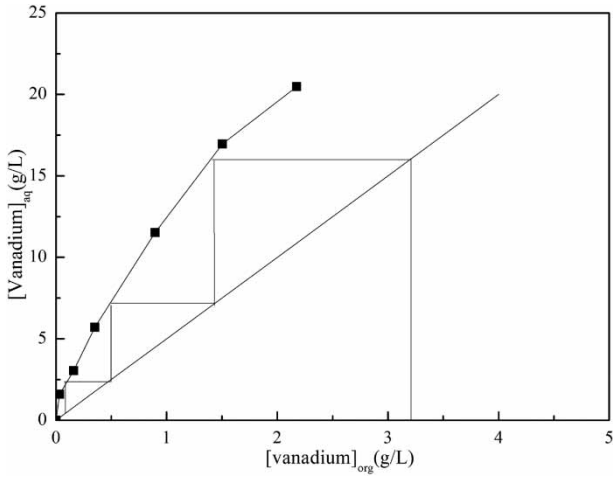

Figure 14 | McCable–Thiele plot for re-extraction of vanadium with $(NH_4)_2CO_3$ from the loaded organic phase.

Table 3 | Chemical composition of raffinate

Element	V	Al	K	Fe^{3+}	Mg
Concentration (g/L)	0.01	1.67	2.64	0.55	2.16

The results indicate that 97.6% vanadium was extracted with extractant 7101 and sec-octyl alcohol, in which 7.1% Al and 14.9% Fe were co-extraction.

Establishment of a separation process for iron and vanadium

The loaded organic phase was always used to extract new solutions up to the saturated state, which contained V of 3.24, Al of 0.31 and Fe of 0.64 g/L. The existence of Al and Fe could seriously affect the re-extraction of vanadium with ammonium carbonate. The hydrochloric acid solution with 4 mol/L was used to wash away Al and Fe impurities more than 80% of Al and Fe were eluted into the acid solution. Re-extraction of vanadium was conducted with 100 g/L ammonium carbonate solution. Different O/A ratios were from 0.5:1 to 20:1 for 8 min. The McCabe-Thiele plot for re-extraction of vanadium with $(NH_4)_2CO_3$ from the loaded organic phase is shown in Figure 14.

Three theoretical extraction stages should be needed at O/A ratio of 5:1, in which 99% vanadium could be re-extracted and the precipitate of ammonium polymer vanadate (APV) was obtained by two phase separation. And then the precipitate was filtered, dried and heated at 520 °C for 60 min. Finally, the product V_2O_5 at 99.5% purity was obtained. Therefore, the following equations can represent the re-extraction of vanadium and the roasting process of ammonium vanadate:

$$(RNH_3)_4H_2V_{10}O_{28} + 3(NH_3)_2CO_3 \rightarrow (NH_4)_6V_{10}O_{28}\downarrow + 4RNH_2 + 3H_2O + 3CO_2\uparrow \quad (10)$$

$$(NH_4)_6V_{10}O_{28} \rightarrow 5V_2O_5 + 3H_2O\uparrow + 6NH_3\uparrow \quad (11)$$

Finally, Figure 15 shows the process flow diagram for the recovery of iron and separation of vanadium from TWWL. More than 97% iron was generated in the form of jarosite with a purity of 99.5%. More than 99% vanadium was extracted using extractant 7101 and sec-octyl alcohols. The product V_2O_5 with 99.5% purity was obtained by washing, re-extraction and heating. Therefore, a feasible and efficient method in an acceptable environment for the recovery of iron and separation of vanadium from TWWL was developed.

CONCLUSIONS

The combined method of crystallization with jarosite and solvent extraction with 7101 was used for recovery of iron and separation of vanadium from TWWL, and the following conclusions were obtained.

(1) More than 97% iron was precipitated with 15 g/L potassium chlorate at a pH of 1.6 at 95 °C for 90 min. The crystallization product was jarosite with purity of 99.5%. Gibbs free energy for jarosite generation was

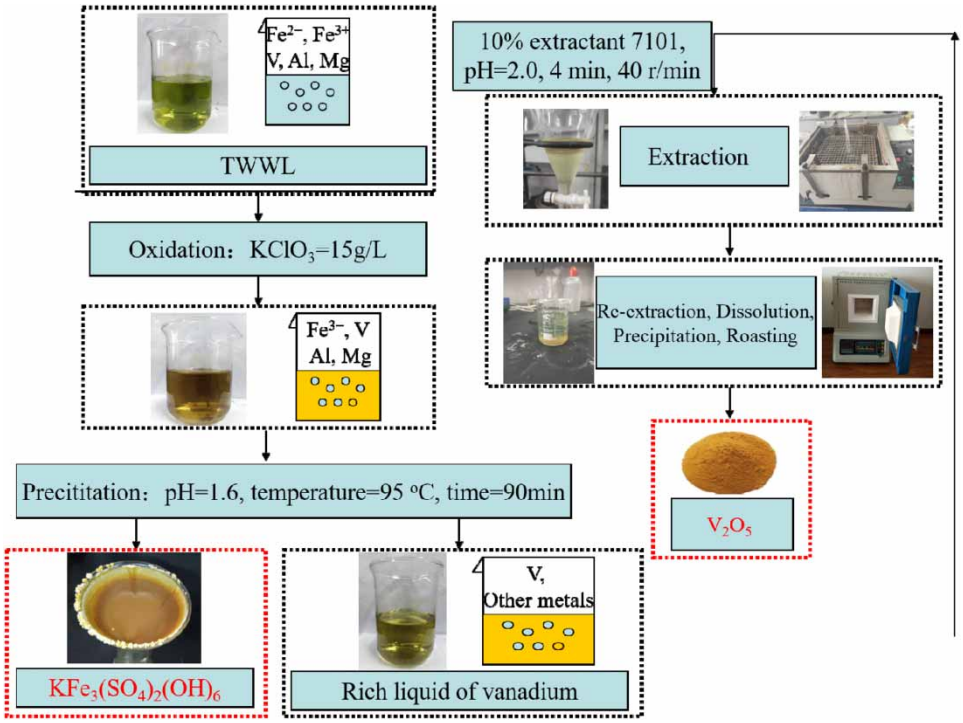

Figure 15 | Flow sheet of separation of iron and vanadium from TWWL.

less than 0 at temperature of 355 K, and the reaction was easily carried out at higher temperatures.

(2) Maximum distribution coefficient (Dv = 7.77) and the vanadium extraction efficiency of 88.6% were obtained at $X_{7101} = 0.5$. The extraction of metal ions occurs in the order V(V) > Fe(III) > Al(III) > Mg(II) > K(I) ≈ Na(I). The $\beta_{(V/Al)}$ and $\beta_{(V/Fe)}$ were 150 and 67, respectively under the conditions of extractant concentration of 20%, pH value of 2.0, extraction time of 4 min and stirring speed of 40 r/min.

(3) Vanadium existed as $H_2V_{10}O_{28}^{4-}$ at pH 2.0, and the NH and C–N groups of extractant 7101 contributed to the extraction of vanadium. Four stages of extraction and three stages of re-extraction were predicated and verified by McCable–Thiele plots. The product V_2O_5 with purity of 99.5% was obtained by washing, re-extraction and heating.

ACKNOWLEDGEMENTS

This research was financially supported by the National Natural Science Foundation of China (51904097 and 51804103), the training program for young backbone teachers in Colleges and Universities of Henan Province (2019GGJS056), Open Foundation of State Environmental Protection Key Laboratory of Mineral Metallurgical Resources Utilization and Pollution Control (HB201905), Scientific and Technological Project of Henan Province (202102310548), Program for Innovative Research Team in the University of Henan Province (21IRTSTHN006).

DATA AVAILABILITY STATEMENT

All relevant data are included in the paper or its Supplementary Information.

REFERENCES

Baccolo, G., Delmonte, B., Niles, P. B., Cibin, G., Stefano, E. D., Hampai, D., Keller, L., Maggi, V., Marcelli, A., Michalski, J., Snead, C. & Frezzotti, M. 2021 Jarosite formation in deep Antarctic ice provides a window into acidic, water-limited weathering on Mars. *Nature Communications* **12**, 1–9.

Calla-Choque, D. & Lapidus, G. T. 2021 Jarosite dissolution kinetics in the presence of acidic thiourea and oxalate media. *Hydrometallurgy* **200**, 105565.

Cui, J. N. & Ren, H. L. 2013 Development and comparison of titanium white production technologies in China. *Rare Metals and Cemented Carbides* **41**, 14–17.

Feng, X., Wu, P. & Jiang, L. Y. 2018 Titanium white waste acid concentration by DCMD: wetting crystallization and fouling. *Desalination* **440**, 112–121.

Feng, M., Wenzel, M., Wang, S. N., Du, H., Zhang, Y. & Weigand, J. J. 2021 Separation of Na_3VO_4 and Na_2CrO_4 from high alkalinity solution by solvent extraction. *Separation and Purification Technology* **255**, 117282.

Guo, S. J., Hong, Y., Jiang, Y. & Ge, R. T. 2020 Solvent extraction of vanadium from leaching solution containing vanadium. *Hydrometallurgy of China* **39**, 309–312.

Hu, P., Zhang, Y. M., Liu, T., Huang, J. & Yuan, Y. 2017 Separation and recovery of iron impurity from a vanadium-bearing stone coal via an oxalic-acid leaching-reduction precipitation process. *Separation and Purification Technology* **180**, 99–106.

Hu, B., Ouyang, J. T. & Jiang, L. Y. 2020 Influence of flocculant polyacrylamide on concentration of titanium white waste acid by direct contact membrane distillation. *Chinese Journal of Chemical Engineering* **28**, 2483–2496.

Jiang, D. D., Song, N. Z., Liao, S. F., Lian, Y., Ma, J. T. & Jia, Q. 2015 Study on the synergistic extraction of vanadium by mixtures of acidic organophosphorus extractants and primary amine n1923. *Separation and Purification Technology* **156**, 835–840.

Li, J. K. & Dai, J. 2014 Research on treatment and utilization of 'Three Wastes' of titanium dioxide production by sulfuric acid process. *Environmental Science* **33**, 63–66.

Li, X. B., Wei, C., Deng, Z. G., Li, M. T., Li, C. X. & Fan, G. 2011 Selective solvent extraction of vanadium over iron from a coal gangue/black shale acid leach solution by D2EHPA/TBP. *Hydrometallurgy* **105**, 359–363.

Li, X. B., Wei, C., Wu, J., Li, M. T., Deng, Z. G., Li, C. X. & Xu, H. S. 2012 Co-extraction and selective stripping of vanadium (IV) and molybdenum (VI) from sulphuric acid solution using 2-ethylhexyl phosphonic acid mono-2-ethylhexyl ester. *Separation and Purification Technology* **86**, 64–69.

Li, W., Zhao, H. & Zhu, X. B. 2018a Experimental study on preparation of jarosite from titanium white waste water. *Rare Metals and Cemented Carbides* **46**, 35–37.

Li, Y. H., Li, Q. G., Zhang, G. Q., Zeng, L., Cao, Z. Y., Guan, W. J. & Wang, L. P. 2018b Separation and recovery of scandium and titanium from spent sulfuric acid solution from the titanium dioxide production process. *Hydrometallurgy* **178**, 1–6.

Liu, W., Yin, Z. F., Li, G. G. & Yang, Y. 2016 Removal of titanium in process of scandium extraction from titanium dioxide waste acid. *Chinese Rare Earths* **37**, 83–89.

Liu, S. L., Zheng, Y. J. & Zhang, S. C. 2017 Recovery of sulfuric acid from titanium white waste acid by diffusion. *Technology of Water Treatment* **43**, 67–84.

Liu, Q. D., Li, M. C. & Xie, K. 2019 Production practice of iron removal by jarosite method from by-product copper sulfate in tin smelting process. *China Nonferrous Metallurgy* **5**, 14–17.

Liu, H., Zhang, Y. M. & Huang, J. 2020a Separation and transfer mechanism of vanadium from black shale leaching solution by supported liquid membrane using n235. *The Chinese Journal of Nonferrous Metals* **30**, 2216–2223.

Liu, Z. S., Huang, J., Zhang, Y. M., Liu, T., Hu, P. C., Liu, H. & Luo, D. S. 2020b Separation and recovery of vanadium and aluminum from oxalic acid leachate of shale by solvent extraction with Aliquat 336. *Separation and Purification Technology* **249**, 116867.

Lu, Y. Z., Huang, Y. J., Huang, R. J., Cen, X. S. & Su, L. M. 2020 An experimental study of removing iron ion from leaching solution of manganese oxide using jarosite process. *China Manganese Industry* **38**, 28–30.

Peng, X. F., Zhang, Y., Zheng, S. L., Fan, B. Q., Wang, X. J., Qiao, S. & Liu, F. Q. 2019 Research progress on separation of vanadium and chromium in solution. *The Chinese Journal of Nonferrous Metals* **11**, 2620–2634.

Rabbani, M. & Ahmadi, A. 2020 Simultaneous removal of iron and sulfate from biodesulfurization solutions of a coking coal by jarosite precipitation. *Journal of Water Process Engineering* **38**, 101678.

Shi, Q. H., Zhang, Y. M., Huang, J., Liu, T., Liu, H. & Wang, L. Y. 2017 Synergistic solvent extraction of vanadium from leaching solution of stone coal using D2EHPA and PC88A. *Separation and Purification Technology* **181**, 1–7.

Song, Y. W. & Wang, H. R. 2019 Using polyvinyl alcohol to improve the deacidification performance of titanium white waste acid: pilot tests. *Waste Management* **87**, 13–20.

Tang, X. N., Chen, X. H. & Xue, A. 2010 Research on leaching kinetics of scandium from red mud. *Hydrometallurgy of China* **29**, 150–155.

Wang, H. J., Feng, Y. L., Li, H. L., Li, H. R. & Wu, H. 2020a Recovery of vanadium from acid leaching solutions of spent oil hydrotreating catalyst using solvent extraction with D2EHPA (p204). *Hydrometallurgy* **195**, 105404.

Wang, L. Y., Zhang, Y. M., Liu, T., Huang, J. & Xue, N. N. 2020b Separation of iron impurity during vanadium acid leaching from black shale by yavapaiite-precipitating method. *Hydrometallurgy* **191**, 105191.

Wei, S. D., Feng, S. J. & Wei, Y. 2007 Summary of treatment and concentration of TiO_2 waste acid. *Organic Chemicals Industry* **39**, 15–17.

Xie, Y. B., Fan, Y. J., Zhang, J. F. & Xie, J. N. 2016 Emulsification and treatment during scandium extraction from titanium white waste acid. *Nonferrous Metals (Extractive Metallurgy)* **12**, 48–50.

Xing, B. L., Zeng, H. H., Huang, G. X., Jia, J. B., Yuan, R. R., Zhang, C. X., Sun, Q., Chen, Z. F. & Liu, B. Z. 2021 Magnesium citrate induced growth of noodle-like porous graphitic carbons from coal tar pitch for high-performance lithium-ion batteries. *Electrochimica Acta* **376**, 138043.

Yang, T., Wang, Z. J., Xiao, J., Liu, J. B., Yu, R. M. & Deng, Z. J. 2015 Study on leaching technology of extraction scandium from red mud and titanium white waste liquid. *Mining and Metallurgy* **24**, 37–40.

Yu, R. M. 2017 Technology of extracting scandium in comprehensive recovery of red mud-titanium white waste acid. *Nonferrous Metals Science and Engineering* **8**, 31–35.

Yuan, J. T. 2017 Scandium extraction process of titanium white waste acid from a certain company in Yunnan. *Mineral Resources and Geology* **31**, 637–640.

Zhang, H. H., Liang, H. L., Fan, Y. J., Huang, T. Y. & Guo, D. Q. 2014 Two-stage neutralization treatment and precipitation

scandium from waste vitriol solution in titanium dioxide production. *Nonferrous Metals (Extractive Metallurgy)* **8**, 45–48.

Zhang, G. Q., Zhang, T. A., Lu, G. Z., Zhang, Y., Liu, Y. & Xie, G. 2015 Extraction of vanadium from LD converter slag by pressure leaching process with titanium white waste acid. *Rare Metal Materials and Engineering* **44**, 1894–1898.

Zhang, W. G., Zhang, T. G., Li, T. T., Lv, G. Z. & Gao, X. J. 2021 Basic research on the leaching behavior of vanadium-bearing steel slag with titanium white waste acid. *Journal of Environmental Chemical Engineering* **9**, 104897.

Zhao, Y. J., Zhang, Y., Xing, W. H. & Xu, N. P. 2005 Treatment of titanium white waste acid using ceramic microfiltration membrane. *Chemical Engineering Journal* **111**, 31–38.

Zhou, J., Yu, Q., Huang, Y., Meng, J. J., Chen, Y. D., Ning, S. Y., Wang, X. P., Wei, Y. Z., Yin, X. B. & Liang, J. 2020 Recovery of scandium from white waste acid generated from the titanium sulphate process using solvent extraction with TRPO. *Hydrometallurgy* **195**, 105398.

Zhu, Z. W., Tulpatowicz, K., Pranolo, Y. & Cheng, C. Y. 2019 Solvent extraction of molybdenum and vanadium from sulphate solutions with Cyphos IL 101. *Hydrometallurgy* **154**, 72–77.

First received 25 December 2020; accepted in revised form 15 March 2021. Available online 24 March 2021